Measurement of sound scattering properties of diffusing panels through the Wave Field Synthesis approach

Angelo Farina, Michele Zanolin, Elisa Crema

Dipartimento di Ingegneria Industriale, Università di Parma,
Via delle Scienze - 43100 PARMA - tel. +39 0521 905854 - fax +39 0521 905705
E-MAIL: farina@pcfarina.eng.unipr.it - HTTP://pcfarina.eng.unipr.it

Abstract

The sound scattering properties of diffusing panels are actually very difficult to measure and to predict. Furthermore, an unique, commonly accepted "diffusion coefficient" has not been defined yet. In this paper the Wave Field Synthesis approach is employed for the experimental measurement of a physically defined diffusion coefficient. The results are in good agreement with the numerical simulations presented in a parallel paper.

1. Precis

Although many researches were conducted in the last few years, a consistent definition of a single number (the "diffusion coefficient") for stating the effectiveness of diffusing panels has not been yet obtained. In this paper, moving from the Wave Field Synthesis approach developed at the Tech. University of Delft, it is demonstrated how it is possible to characterize completely the scattering properties of a generic object by a large number of impulse response measurements taken moving the microphone at small steps along a straight line. From this characterization, by comparison with the theoretical behaviour of an absorbing/diffusing object, and after separation of the edge diffraction effect, it is possible to define objectively a surface diffusion coefficient. This new quantity is easy to measure, and ranks correctly diffusing panels of various kinds. Furthermore, this new approach is consistent with the employment of the measured diffusion coefficient in room acoustics simulation programs based on the geometrical acoustics theory, as reported in a parallel paper. The work starts with the theoretical explanation of the method, and prosecutes with experimental measurements on different panels, with validation of the results by comparison with numerical simulations.

2. Introduction

The actually employed methods for measuring the scattering properties of objects are based on a series of measurements taken placing microphones on a semicircumference (or on a hemisphere) centered in the center of the object under test. This way, results suitable for the construction of polar patterns are easily obtained.

Furthermore, the “spatial uniformity” of the scattered sound energy can easily be evaluated: the recently proposed “diffusion uniformity coefficent” [1,2] is an unique numeric descriptor of such an uniformity. After having evaluated the impulse response in each j-th of the N microphones, separated the reflected signal from the incident one, and computed the “intensity” I_j as summation of the squared pressure values, the definition of the uniformity coefficient is as follows:

$$\delta_{uc} = \frac{\left(\sum_j I_j\right)^2 - \sum_j \left(I_j{}^2\right)}{(N-1)\cdot \sum_j \left(I_j{}^2\right)}$$

This parameter is usually evaluated for each frequency band, and ranges from 0 (the sound is scattered back only in a very narrow angle) to 1 (the reflected sound is spread uniformly over the whole hemispace). The above definition inherently assumes as "perfect diffusion" an uniform re-irradiation, not a Lambert re-irradiation as it is commonly accepted in thermal sciences for radiant exchange.

In practice, the above approach is satisfying for the comparison of different diffusing panels, as it ranks correctly the "diffusion quality" of various surfaces at least from an energetic point of view.

But the "diffusion uniformity coefficient" is not directly corresponding to the "quantitative" diffusion coefficient usually introduced in room acoustics programs, where an empiric definition is usually accepted:

$$\delta = \frac{\text{energy reflected in a diffuse way}}{\text{total reflected energy}}$$

In which it is assumed that the total reflected energy is composed of two parts: the specular one, which goes in the specular direction, defined by the Snell's law, and the diffused energy, which spread uniformly in all the directions.

The above two definitions of the diffusion coefficient δ are almost coincident for the extremes of the scale: a flat, polished panel for which is $\delta=0$ will be probably measured with very little values of δ_{uc}, and instead an highly diffusing surface, with an almost uniform polar pattern of the reflected intensity will give unitary values for both coefficients.

But in intermediate cases, the qualitative nature of the first coefficient and the quantitative nature of the second cause intrinsic mismatch between the values. Consider first the case of a panel which scatters the sound in all directions, but with pronounced lobes which modulate the radiation of the diffused energy between a constant maximum and zero. In this case, the amount of energy which goes in the "specular" direction is negligible, and thus δ approaches 1, whilst δ_{uc} is approximately 0.5.

Consider then the opposite case of a panel which exhibit an evident specular behavior, so that 70% of the reflected energy goes in the specular direction corresponding with the Snell's law. But the other 30% of the reflected energy is spread uniformly in all directions. In this case, by definition, δ is 0.3, but instead the value of δ_{uc} depends on the geometry of the measurement setup. In fact, the ratio between the distance between the panel and the sound source (d_{source}), and the distance between the panel and the microphones (d_{mic}) influences the ratio between the specular intensity and the diffused intensity, and so the value of δ_{uc} can assume almost any value.

This was checked by numerical simulation of a test case, in which an omnidirectional point source is located at a distance r_1 = 10 m, in front of the panel (θ=90°), whilst a semicircular array of 37 microphones (spaced 5°) is surrounding the diffusing panel, at a distance r_2=5m,. The size of the panel is assumed to be 1m x 1m (S_{panel} = 1 m^2) and thus it intercepts a fraction $S_{panel}/(4\pi r_1{}^2)$ of the total radiated sound power W. The absorption coefficient is assumed zero. The specularly-reflected sound intensity received by the three microphones in the specular zone (the central one and the two adjacent) is:

$$I_{spec} = \frac{W \cdot (1-\delta)}{4 \cdot \pi \cdot (r_1 + r_2)^2}$$

Instead, the diffuse sound intensity received by all the microphones (including the three central ones, where it sums to the above specular intensity) is:

$$I_{diff} = W_{inc} \cdot \frac{\delta}{2 \cdot \pi \cdot r_2^{\,2}} = \frac{W \cdot S_{panel}}{4 \cdot \pi \cdot r_1^{\,2}} \cdot \frac{\delta}{2 \cdot \pi \cdot r_2^{\,2}}$$

Fig. 1 reports the results of the above calculation of sound when the "true" diffusion coefficient δ is 0.3. From such a distribution of sound intensities, the "diffusion uniformity coefficient" δ_{uc} can be computed following its definition: it resulted equal to 0.061426, which is quite different from δ. This computation was repeated for different values of δ: fig. 2 reports the results of this simulation, from which it is clear that δ_{uc} and δ are related by a not-linear relationship, which depends on the geometry of the case studied, and particularly on the number of microphones which happen to fall inside the specular zone.

It must be noted that the relationship reported in fig. 2 cannot be considered general, it is valid only for the particular geometric case depicted above.

The result of this preliminary analysis is that the recently proposed diffusion uniformity coefficient [1,2], although easily measurable and certainly well correlated with the acoustical properties of different diffusors, is not corresponding with the "quantitative" diffusion coefficient usually implemented in computer programs for the prediction of the sound field in large enclosures [3].

The main goal of this research is consequently to develop a measurement technique and a subsequent data analysis procedure, capable of estimating the "true" value of the diffusion coefficient, so that introducing it in room acoustics programs produces correct results.

3. The Wave Field Synthesis (Analysis) approach

Wave Field Synthesis was initially developed at the Tech.University of Delft as a technique for producing synthetic sound fields, thanks to linear arrays of loudspeakers [4]. More recently, the technique was folded back to the analysis of complex sound fields, being renamed Wave Field Analysis [5]. In this second application, a large number of impulse responses are measured with a single microphone, repeatedly placed in subsequent positions along a straight line, with constant spacing.

After the impulse responses are measured, an image is formed plotting the magnitude of the signal along a vertical line for each microphone in terms of darkness of the pixels. This graphing technique is common in other fields, such as underwater acoustics or medical imaging. Important information can then be obtained applying to such images proper data processing techniques, the most simple being windowing and filtering, going up to deformations and synthetic focusing.

In the case of a diffusing panel inserted in a flat surface, this technique evidences the scattered wavefronts from the specularly reflected one, as the first has more curvature than the latter [6]. In principle, this different curvature could be used for separating the two sound fields (specular and diffused), and this would enable the direct computation of the "true" diffusion coefficient.

So it was decided to employ a data acquisition technique based on the WFS approach, with a microphone moving along a straight line instead of along a semicircumference. As it will be explained in the following paragraphs, this made it possible to obtain a better understanding of the reflected sound field than what can be seen by energetic polar plots. Although the direct computation of the diffusion coefficient with WFS is not finished yet, the

first results obtained with the new technique are so promising that it was decided to publish this preliminary paper, with the goal to promote the debate about the correct definition of the diffusion coefficient and about the possible measurement techniques.

4. Experimental apparatus

Two experimental setup were employed for this work. In the first one, the diffusing panel was placed on an hard, polished concrete floor, and a loudspeaker was suspended above it. The experiment was conducted in a large, untreated room: the elimination of unwanted reflection was obtained by time windowing of the measured impulse responses.

An omnidirectional microphone was moved along a line, passing over the diffusing panel, thanks to a light carriage and a rotating board which acted as drum, over which a cable was folding pulling the carriage. A rail embedded in the floor ensured linear movement of the microphone. The advancement step was 27.91 mm, and 255 microphone positions were measured.

The measurement was conducted with a PC equipped with a MLSSA board, directly interfaced with the rotating board. A macro ensured automatic, unattended operation (the whole measurement procedure was lasting more than three hours).

Fig. 3, 4 and 5 show the overall setup, the suspended loudspeaker, the rotating board and the panel on the floor. As shown, it was attempted to reduce the unwanted reflections from the carriage by covering it with a thick coat of sound absorbing material, which gained it the surname of “sheep”.

Fig. 6 shows a typical result obtained from a measurement conducted with the first apparatus. It can be seen that the specular reflection on the floor causes a very evident, low-curvature wavefront, whilst the sound diffused from the panel distributes over a much more curved wavefront. As these wavefronts are crossing, it was not easy to separate the two contributions. Some attempts to operate a spatial separation of the wavefronts failed, although a lot of time was wasted writing Matlab programs.

So it was decided to make the things easier, modifying the experimental apparatus in such a way to avoid completely the specular reflection on the floor. The relative position of loudspeaker and diffusing panel was interchanged: the loudspeaker was mounted flush on the floor, in which a proper niche was created. The diffusing panel was suspended above it.

Also the measurement equipment was updated: a new computer, fitted with an high-quality Echo Layla sound board was employed (capable of simultaneous acquisition of up to 8 channels, at 20 bit), and the omnidirectional microphone was substituted with a three dimensional pressure/velocity probe (a Soundfield MKV microphone), sampling simultaneously its four channels (pressure and the three cartesian components of the particle velocity). This was possible thanks to the measurement software Aurora [7], employed in its multiple-MLS mode (emulating the MLSSA board).

Although these acquisition make it possible, in principle, to measure the three-dimensional sound intensity, only the pressure channel results were employed for the subsequent computations till now: in the future, a more robust true intensimetric analysis will be conducted on the acquired data, instead of employing the squared pressure in place of the true acoustic intensity.

Figs. 7 and 8 show the second measurement setup with particulars of the microphone and loudspeaker.

The second measurement setup revealed capable of producing much more clean images. It was also possible, thanks to the advanced digital signal processing tools included in Aurora, to apply a proper filtering to the measured impulse responses, for “sharpening” the time signature of the loudspeaker. This was possible thanks to the module which computes the

Nelson/Kirkeby inverse filter of the loudspeaker response [8], which was computed selecting the direct wave in the microphone located exactly above the loudspeaker. After the computation of the inverse filter, it was applied by convolution to the whole sequence of 255 impulse responses, obtaining a substantial deconvolution of the loudspeaker signature to an almost perfect Dirac's delta function.

This process was capable of producing a substantial improvement of the image definition, as it is demonstrated in fig. 9, which compares an original acquisition with the corresponding filtered image. Thus the same processing was systematically employed for all the measurements conducted with the experimental apparatus #2. A further improvement is possible, substituting the MLS signal with the new logarithmic sweep [9]. This method was not employed here because it takes more time for the processing, although it is planned to repeat all the measurements also with this new technique, which already demonstrated to produce better results particularly regarding the peak sharpness and the S/N ratio.

5. Results from the tests on three diffusors

In the following, the results obtained with three different diffusing panels are presented. The first one is a square, flat, smooth panel, made of heavy wood (MDF) and measuring 0.715 x 0.715 m. The second has the same size and is made of the same material, but has evident diffusing properties at medium frequency due to its construction as a sequence of cavities of different depth (it is visible in fig. 5). The third is a curved hemicylinder, also made of smooth wood (marine plywood), measuring 2m x 0.9m. It was measured in the direction of maximum diffusion, that is perpendicularly to the cylinder axis.

Fig. 10 shows the three WFS representations of the measurement on these three panels, after the Kirkeby equalization.

The next step in processing the experimental results was the separation of the direct sound from the reflected waveform. This was possible employing the WFS theory for computing proper spatial windows, and applying them to the above results, setting to zero all the data points outside these windows.

This process is possible on a simple geometrical basis, as the computation of the traveled distance translates easily in the corresponding time lag over the impulse response of each microphone. The windowing process is demonstrated in fig. 11. The experimental response of the curved panel is separated in the direct and reflected parts; the plots of the latter two data-sets have been done with a wider dynamic range (150 dB instead of 100 dB), so that the exact shape of the windows is made evident.

After the windowing, it is possible also the "listen" separately at the direct and reflected sound. The first is always the same for all the measurements, whilst the second reveals the nature of the reflected sound. In fact, the flat panel produces a short impulse (but somewhat smeared for the border effect), the diffusing panels responds with a smooth and long signal, having little impulsive character, and the curved surfaces produces a very sharp peak, without any sort of tail. This different behavior is evident looking at fig. 12, which shows the enlarged portion of the reflected waves for the central microphone.

6. Evaluation of the diffusion uniformity coefficient

In its original formulation, the diffusion uniformity coefficient has to be evaluated from measurements of the reflected component made with microphones placed along a circular arch, centered in the middle of the panel. In our measurements, instead, the microphones are placed at varying distance from the center of the panel. So it is necessary to compensate for this varying distance, assuming spherical divergence from the center of the panel.

If the distance of the panel from the floor is called z_c, the distance of the microphones from the floor is called z_r, and the current position of each microphone is called x (with x=0 above the loudspeaker), the reflected intensity of each microphone can be corrected as follows:

$$I_{semicircle} = I_{line} \cdot \left(\frac{(z_c - z_r)^2 + x^2}{(z_c - z_r)^2} \right)$$

The angle is then related to the longitudinal position of the microphone with the relationship:

$$\varphi = \arctan\left(\frac{x}{z_c - z_r} \right) + \frac{\pi}{2}$$

With this kind of post processing, the polar pattern of the reflected energy can be constructed for each of the three panels.

This computation can be repeated at many frequencies, obtained by proper filtering in octave bands of the windowed impulse responses. Figs. 13, 14 and 15 show the polar patterns at 8 frequencies for the three panels. In fig. 15 it is easy to see how, being the cylindrical diffuser a not-isotropic scatterer, which spreads the sound more in a cylindrical way than in a spherical one, the application of the above equation for spherical correction causes the extreme microphones to be over-corrected, and the polar pattern seems to indicate that more sound is redirected at very low or very high angles than near the specular direction.

From each polar pattern it is quite easy to compute the diffusion uniformity coefficient, making use of the normalized autocorrelation definition provided in [1,2] and already discussed in the paragraph 2 of this paper (it is the first formula). Figs. 16, 17 and 18 show the frequency spectrum of the diffusion uniformity coefficient for the three tested panels.

It is evident how this uniformity parameter assigns maximum values to the smooth behavior of the curved panel, although the reflected sound coming from it sounds very “specular”. This must make it clear that the diffusion uniformity coefficient is “qualitative” in the sense that it relates to the overall quality of the sound diffusion, it does not have any relationship with the temporal structure of the reflected sound and its intrinsic coherence.

7. Estimation of the quantitative diffusion and absorption coefficients

As the derivation of the quantitative diffusion coefficient (as the ratio between the diffused energy and the total reflected energy) revealed to be quite difficult, it was decided for now to search for approximate values of the “true” diffusion coefficient. The separation of the diffused and specular reflected intensities will be probably possible working with the true intensimetric measurements, following the theory already developed in [10] for the measurement of the absorption coefficient.

The approximate definition of the diffusion coefficient is very pragmatic: we search for the value of the diffusion coefficient (and of the absorption coefficient, at once) which, inserted in a simplified formulation of the reflection (specular, diffuse, and border effect) produces numerical results in optimal agreement with the experimental ones.

The theory for the computation of the diffuse reflections has been derived in a parallel paper [3], so here we report only the final results. Considering the geometrical assumptions depicted in fig. 19, at each microphone position, the total diffused energy which comes back from the panel can be computed as:

$$I_{diff} = \int_{y=-b}^{b} \int_{x=-a}^{a} \frac{W \cdot z_c}{4 \cdot \pi \cdot r_1^3} \cdot \frac{(1-\alpha) \cdot \delta_{loc}}{2 \cdot \pi \cdot r_2^2} \cdot dx \cdot dy$$

In which δ_{loc} is the local value of the diffusion coefficient, due to the increase of the diffusion coming near to the edges of the panel. In practice, δ_{loc} increases over the normal value of δ only starting from a distance equal to $\lambda/2$ from the border of the panel, and it reach its maximum value (1) at the border itself, following this linear equation:

$$\delta_{loc} = 1 - (1-\delta) \cdot \frac{d_{min}}{\lambda / 2}$$

The analytical computation of the above integral is not easy, so it was decided to perform it numerically, inside an Excel spreadsheet. The surface of the panel was divided in 11x11 cells, and from each cell a local contribution to the diffused energy is computed for each microphone. This way, a column of 255 theoretical reflected intensities is obtained, and this is compared with the column containing the experimentally measured values of the reflected intensity.

First of all, the value of the emitted sound power W is adjusted so that the direct wave, for the central microphones, assumes exactly the same value as measured. Thereafter, the Excel's solver function is employed, for automatically optimizing the values of α and δ which cause the numerical results to maximally match the experimental data. This process takes some minutes, and after the optimization is concluded it is possible to compare graphically the results.

Figs. 20, 21, 22 and 23 show the results obtained for the three already described panels, and for a fourth one which is simply the same curved panel already employed, but turned in it direction of minimum diffusion (with the cylinder axis parallel to the microphone array).

This table compares the values of the diffusion coefficients with the diffusion uniformity coefficient, at the frequency of 1 kHz.

Parameter	Flat Panel	Galav2 diffuser	curved panel	curved panel (90°)
α	0	0.03	0.286	0.76
δ	0.117	0.86	1	0.20
δ_{uc}	0.35	0.86	0.92	0.52

It can be seen that in some cases the correspondence is very good, but in others the values of δ and δ_{uc} are very different.

8. Conclusions and future work

In this paper it was demonstrated that the recently proposed definition of a diffusion uniformity coefficient produces values which are effectively significant for the qualification of diffusing panels, and correctly ranks their capabilities at various frequencies.

Nevertheless, it resulted that the values of this "diffusion uniformity" coefficient are not always satisfying for the numerical computations made under the hypothesis of geometrical acoustics: the experimental results are often better explained with a value of the "true" diffusion coefficient (also called quantitative diffusion coefficient) which can differ significantly from the uniformity coefficient.

The experimental apparatus developed for this research made it possible to employ some parts of the Wave Field Synthesis theory: this revealed particularly useful for obtaining a graphical representation of the scattered wavefronts, but also for the separation of the direct

and reflected waves. In principle, with similar techniques it could be possible to separate the diffuse from the specular reflections, and this remains a topic on which further research is required.

A second improvement in the data analysis procedure will be the use of the complete measured data sets, including the particle velocity components, so that the true sound intensity vector can be computed in each measurement point.

Finally, the experimental basis will be enlarged, repeating measurements on a wider number of different scattering objects.

9. Acknowledgements

This work was supported by a research convention with Audio Link – Alberi (Parma), Italy and from the Italian Ministry for University and Research (MURST) under the grant MURST-98 #9809323883.

10. References

[1] T.J. Hargreaves, T.J. Cox, Y.W. Lam, P. D'Antonio, "Characterising scattering from room surfaces", proc. 16th ICA and 135th Meeting A.S.A., Seattle WA, vol. IV, pp2731-2732, June 1998.

[2] P. D' Antonio, T. Cox, "Two Decades of Sound Diffusor Design and Development" (part 1 and 2) Journal of AES vol. 46, n° 12 (December 1998).

[3] A. Farina, "Introducing the surface diffusion and edge scattering in a pyramid-tracing numerical model for room acoustics", Pre-prints of the 108th AES Convention, Paris, 19-22 February 2000.

[4] A. J. Berkhout, P. Vogel, D. de Vries, "Use of Wave Field Synthesis for Natural Reinforced Sound" – Pre-prints of the 92th AES Convention, #3299, March 1992

[5] D. de Vries, A. J. Berkhout, J. J. Sonke, "Array Technology for Measurement and Analysis of Sound Fields in Enclosures" - Pre-prints of the 101th AES Convention, #4266, May 1996.

[6] Diemer de Vries and Jan Baan, "Auralization of Sound Fields by Wave Field Synthesis" - Pre-prints of the 106th Convention, Munich, Germany, 1999 May 8–11, # 4927.

[7] A. Farina, F. Righini, "Software implementation of an MLS analyzer, with tools for convolution, auralization and inverse filtering", Pre-prints of the 103rd AES Convention, New York, 26-29 September 1997.

[8] O. Kirkeby and P. A. Nelson – "Digital Filter Design for Virtual Source Imaging Systems", Pre-prints of the 104th AES Convention, Amsterdam, 15 - 20 May, 1998.

[9] A. Farina, "Simultaneous measurement of impulse response and distortion with a swept-sine technique", Pre-prints of the 108th AES Convention, Paris, 19-22 February 2000.

[10] A. Farina, A. Torelli - "Measurement of the sound absorption coefficient of materials with a new sound intensity technique" - Pre-prints of the 102nd AES Conference, Berlin, 23-26 March 1997.

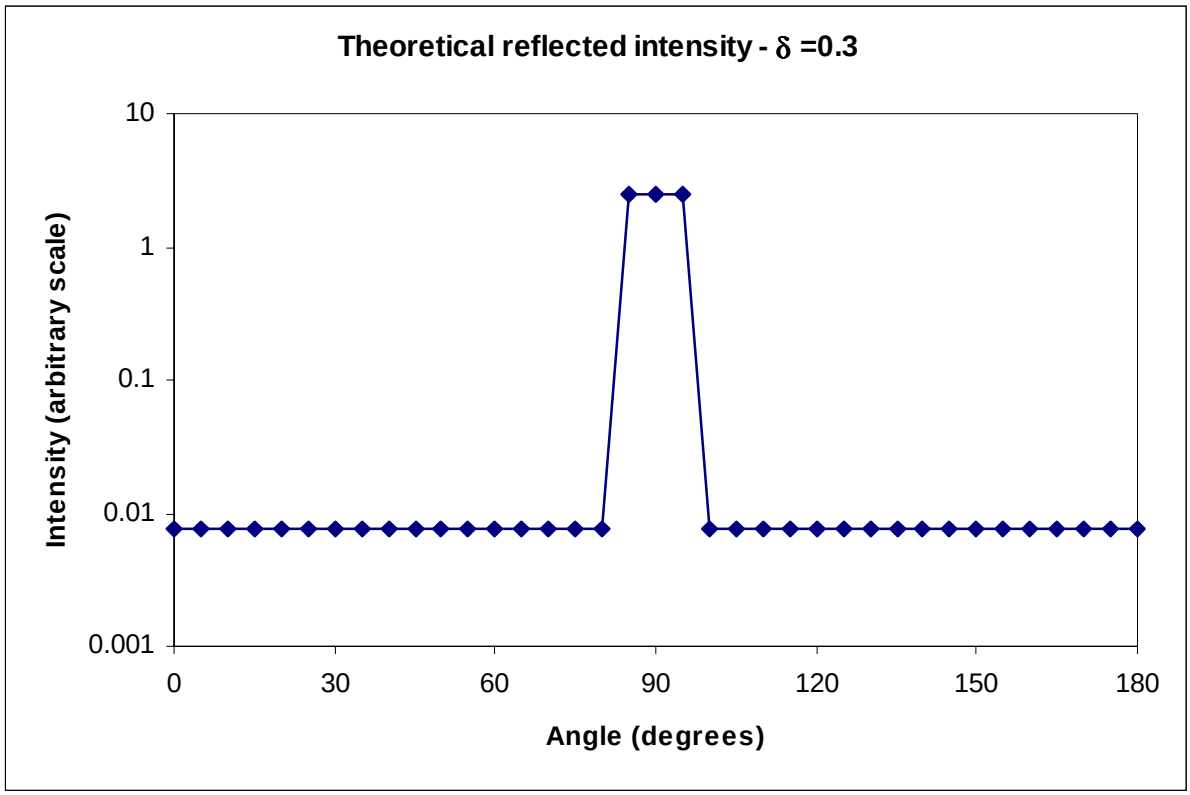

Fig. 1- Theoretical angular distribution of the intensity reflected by a 1m•1m panel with δ=0.3

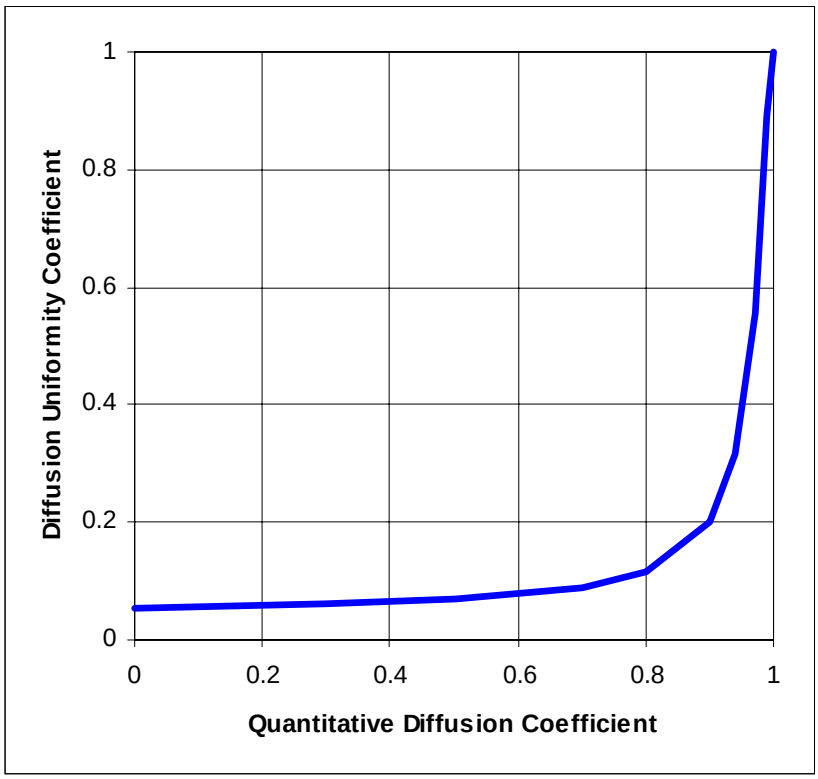

Fig. 2 – Theoretical relationship between quantitative diffusion coefficient δ and qualitative diffusion-uniformity coefficient δ_{uc}.

Fig. 3 – experimental apparatus #1, overall view

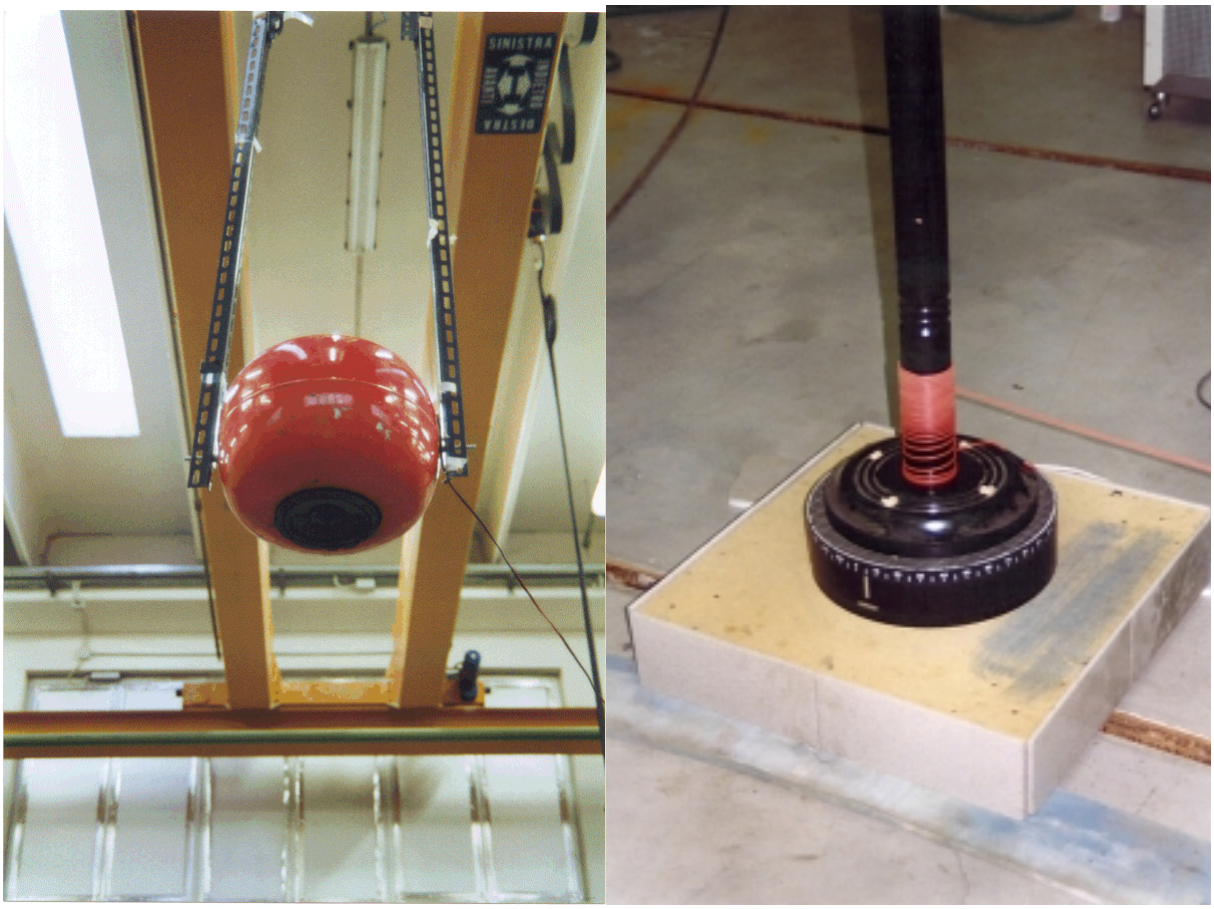

Fig. 4 – Experimental apparatus #1, particular of the suspended loudspeaker (left) and of the rotating board with the cable folding around the drum (right).

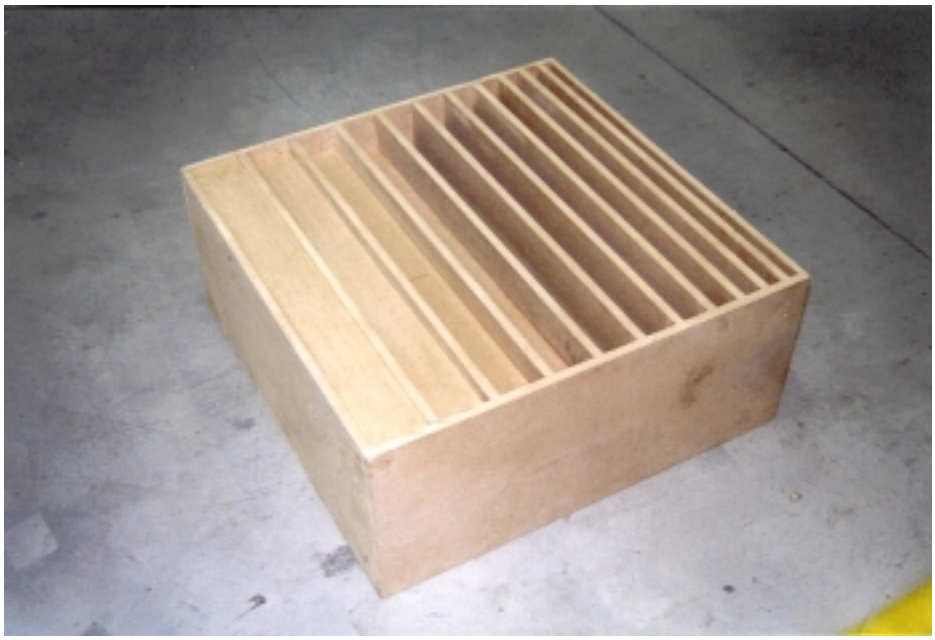

Fig. 5 – the diffusing panel (named GALAV2) on the reflecting floor.

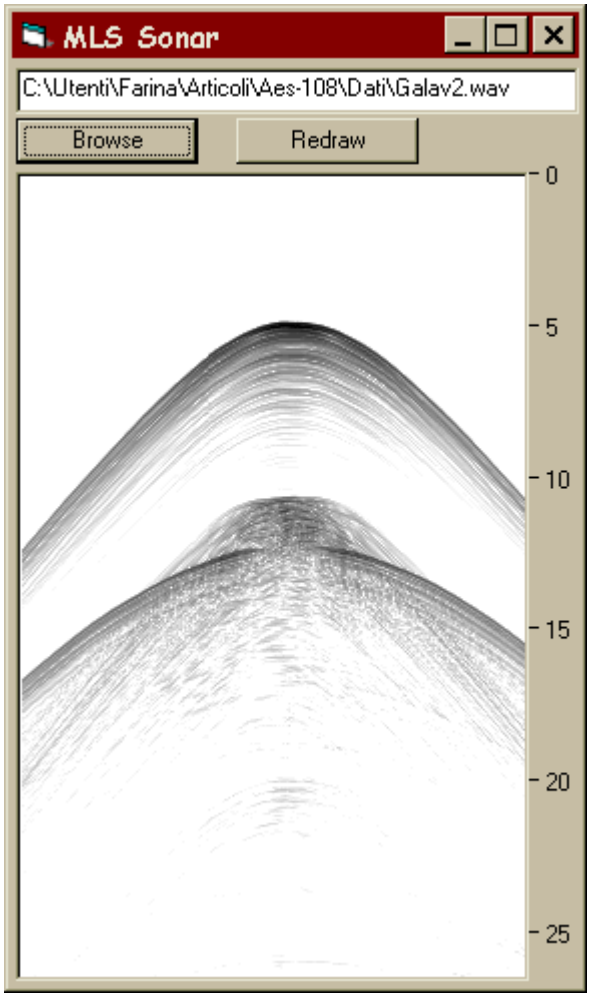

Fig. 6 – Sonar result with experimental apparatus #1

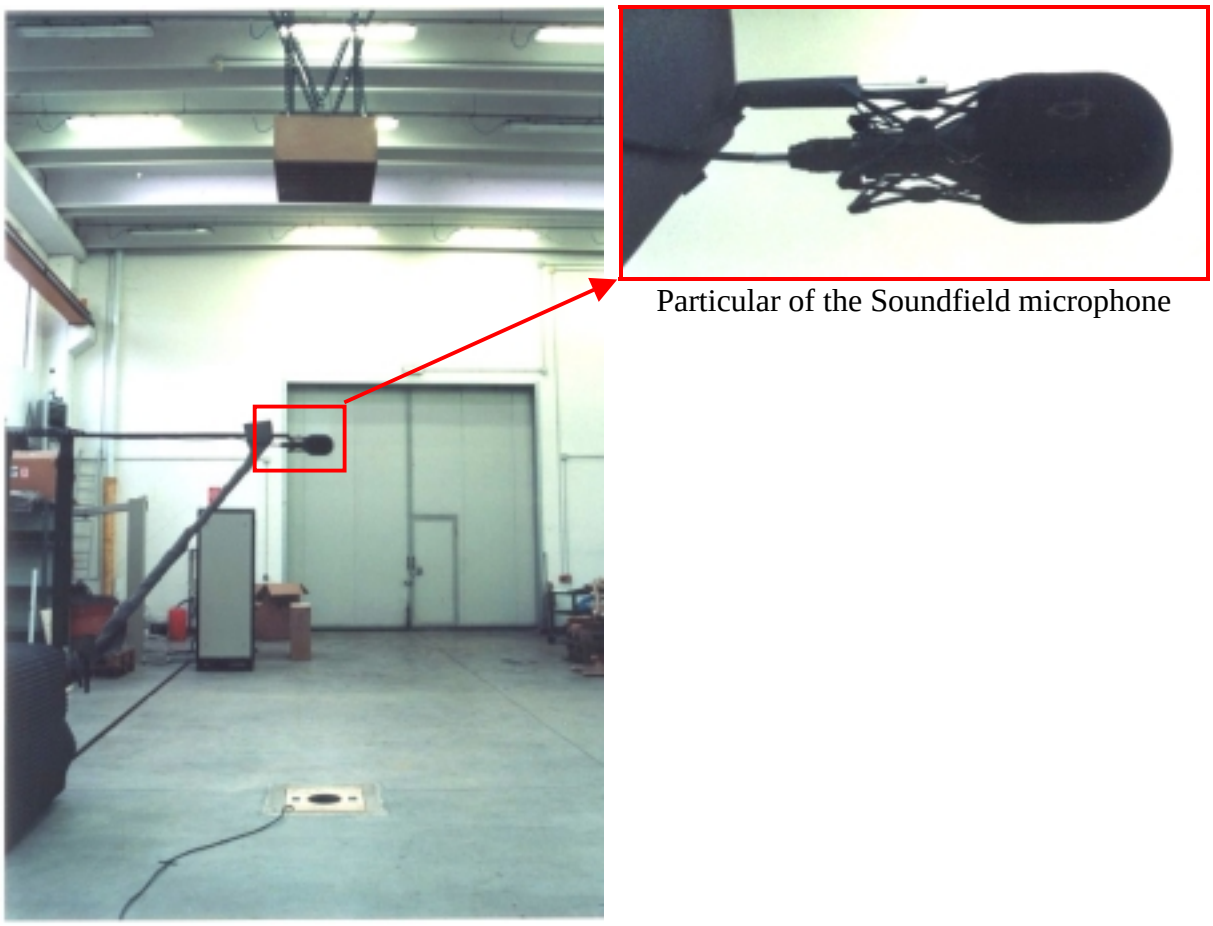

Fig. 7 – Experimental apparatus #2 – Overall view

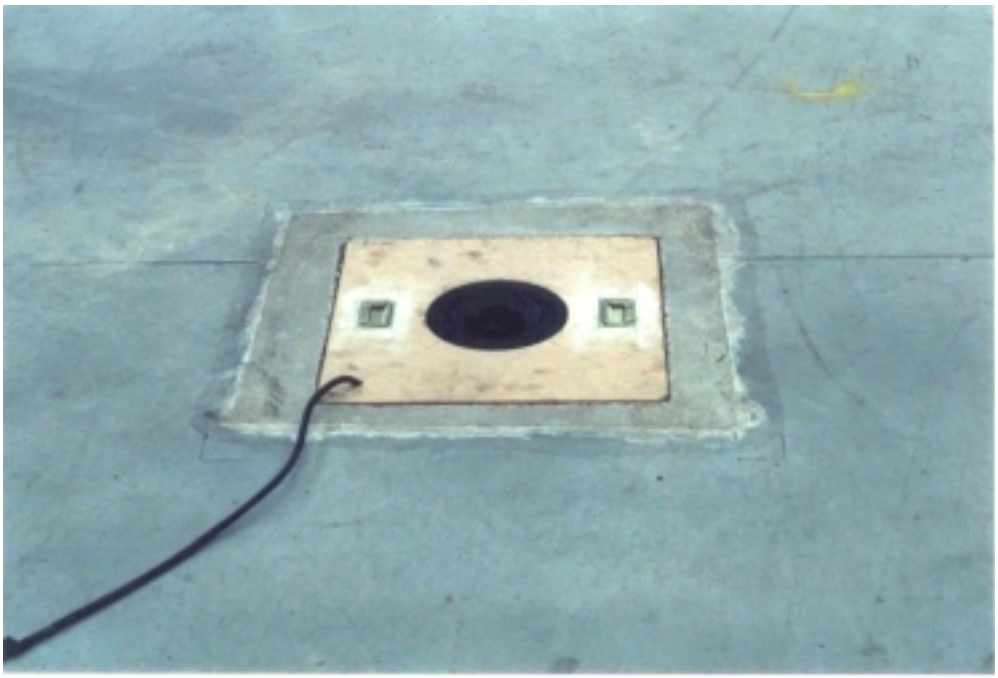

Fig. 8 – Particular of the loudspeaker inserted in the floor

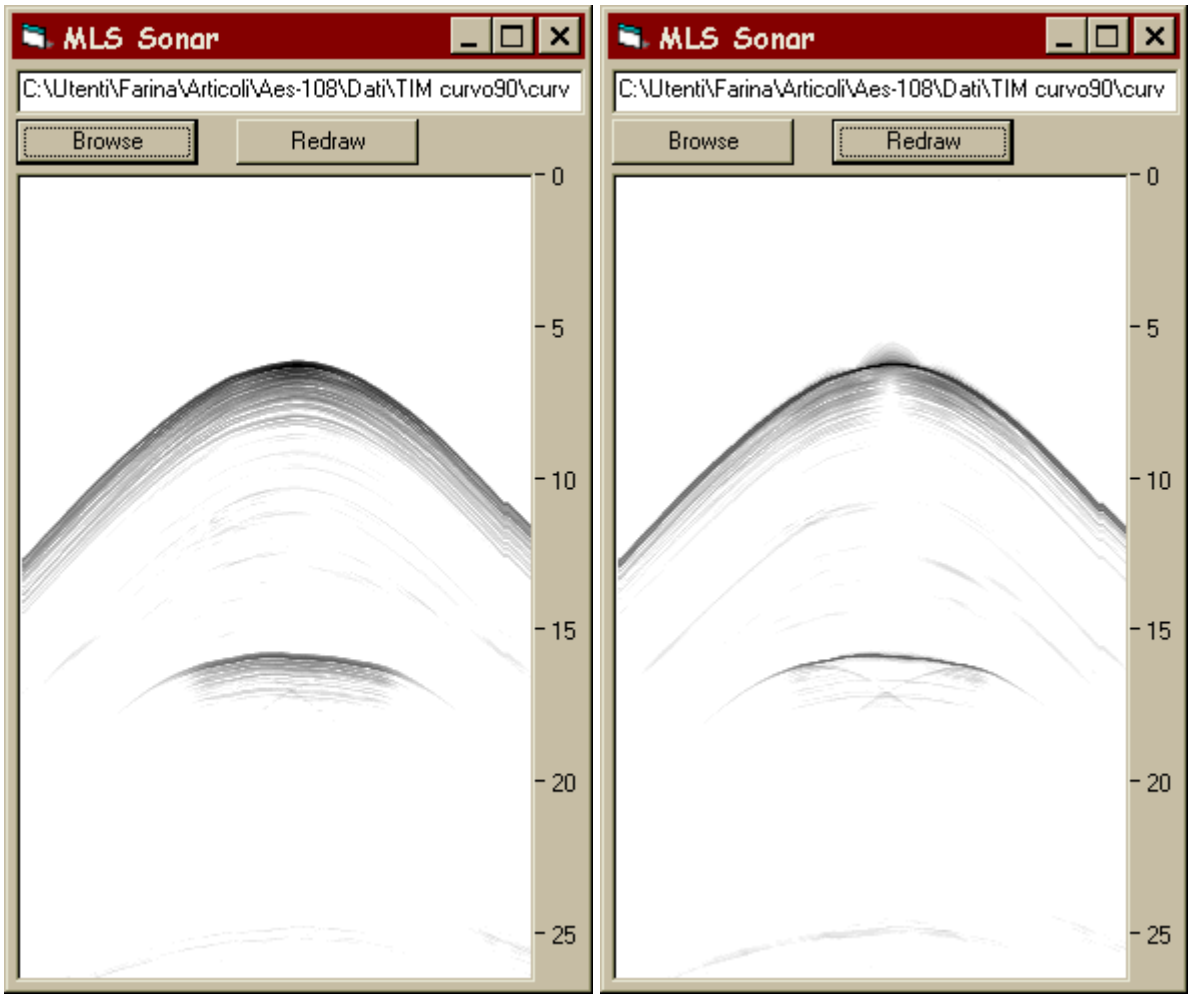

Fig. 9 – Measurement with apparatus #2, original (left)
and after convolution with the Kirkeby inverse filter (right)

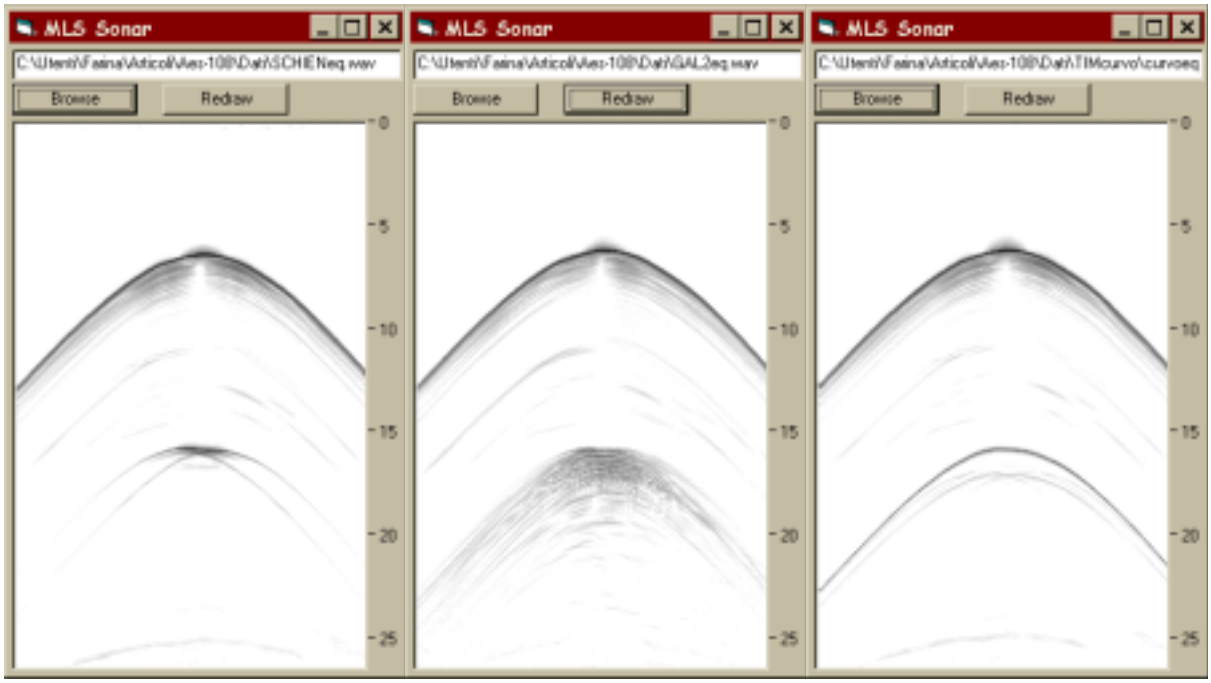

Fig. 10 – responses of three different panels

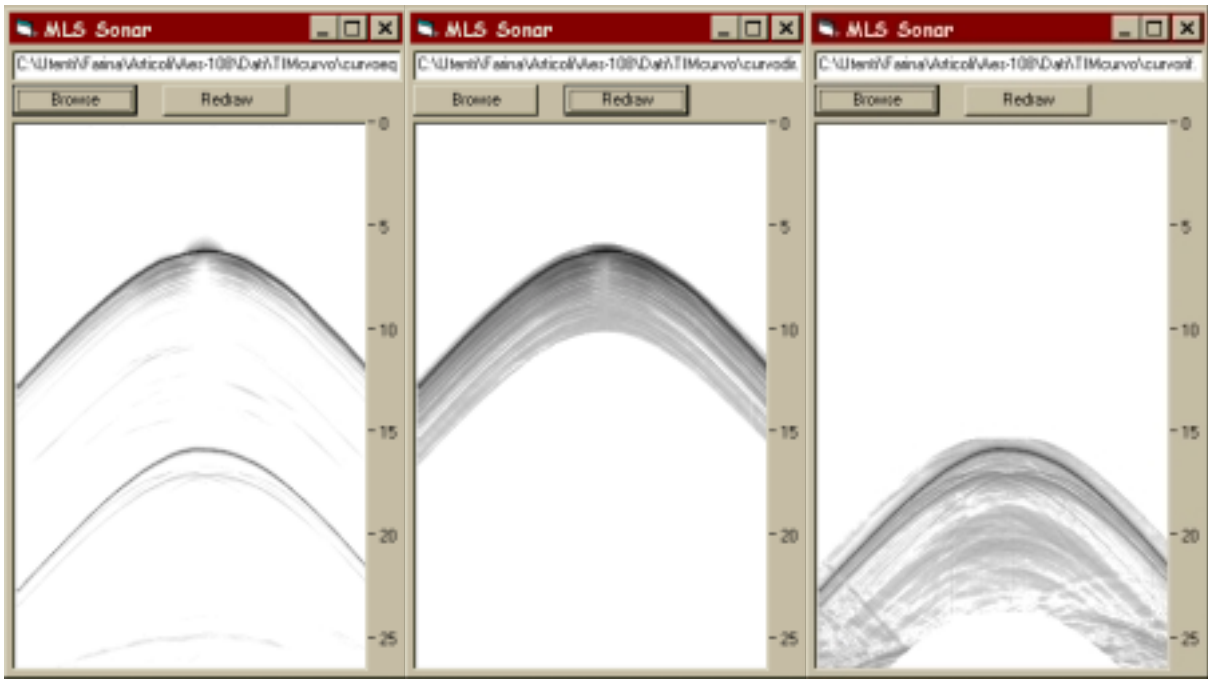

Fig. 11 – windowing of the original signal (left) in the direct (center) and reflected (right) components

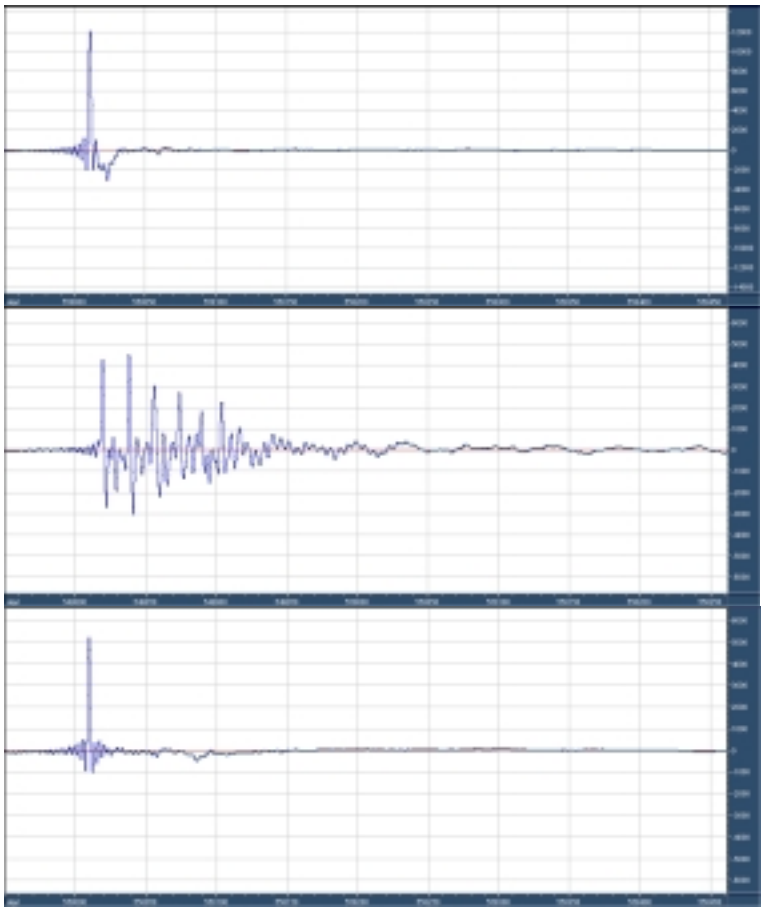

Fig. 12 – Waveform of the reflected signals – Flat panel (above), diffusing panel (middle), curved panel (below)

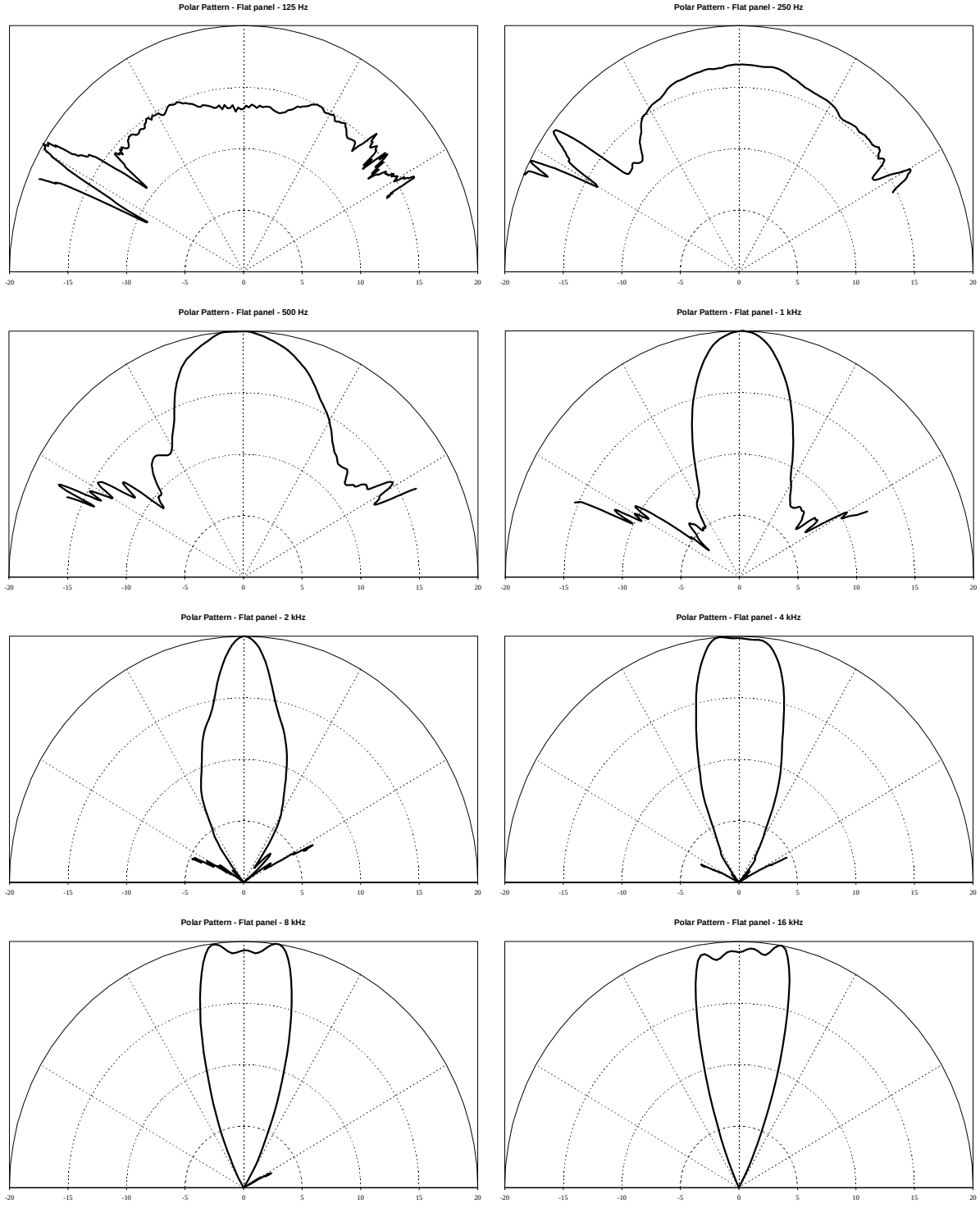

Fig. 13 – Polar patterns of the flat panel

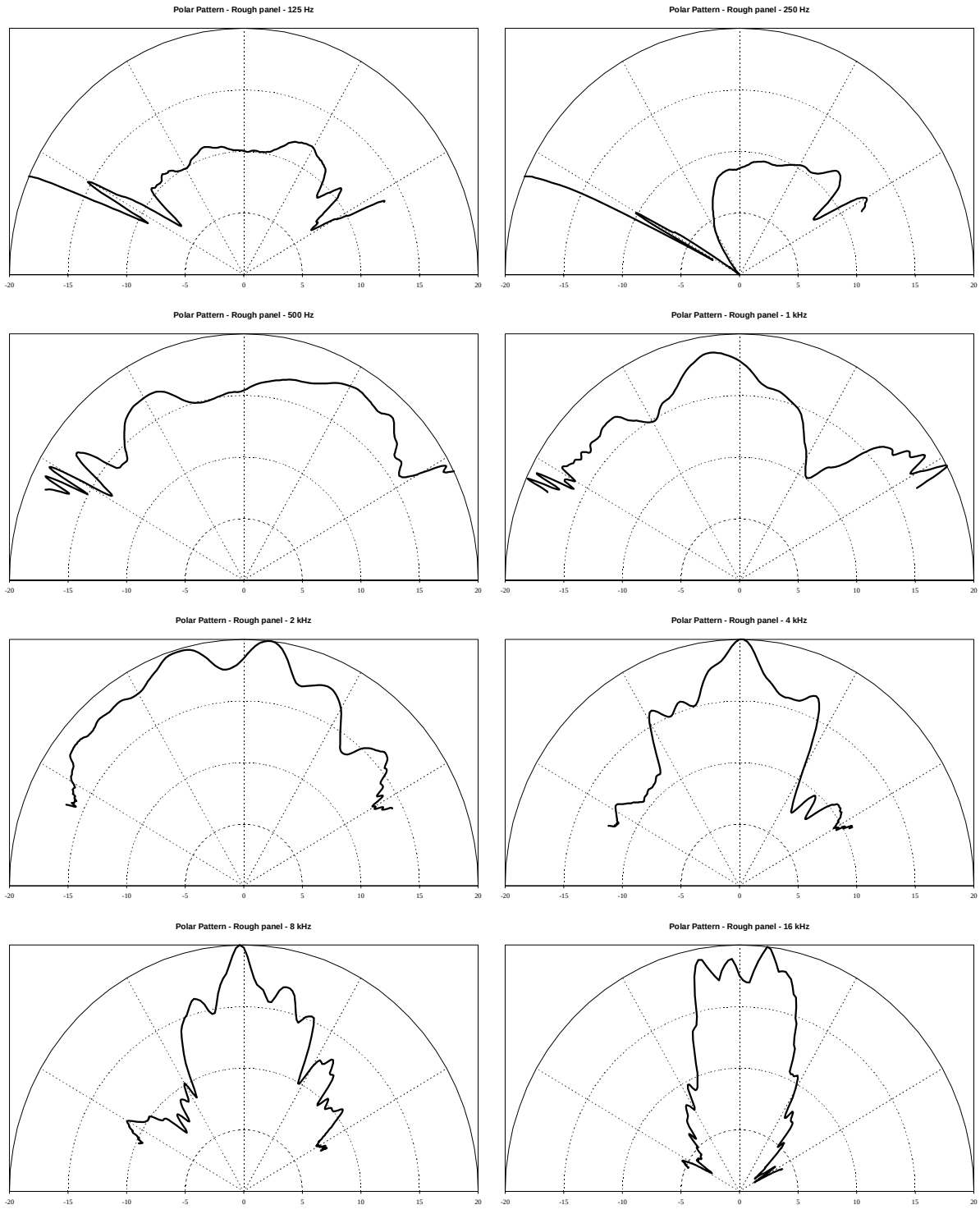

Fig. 14 – Polar patterns of the GALAV2 diffusing panel

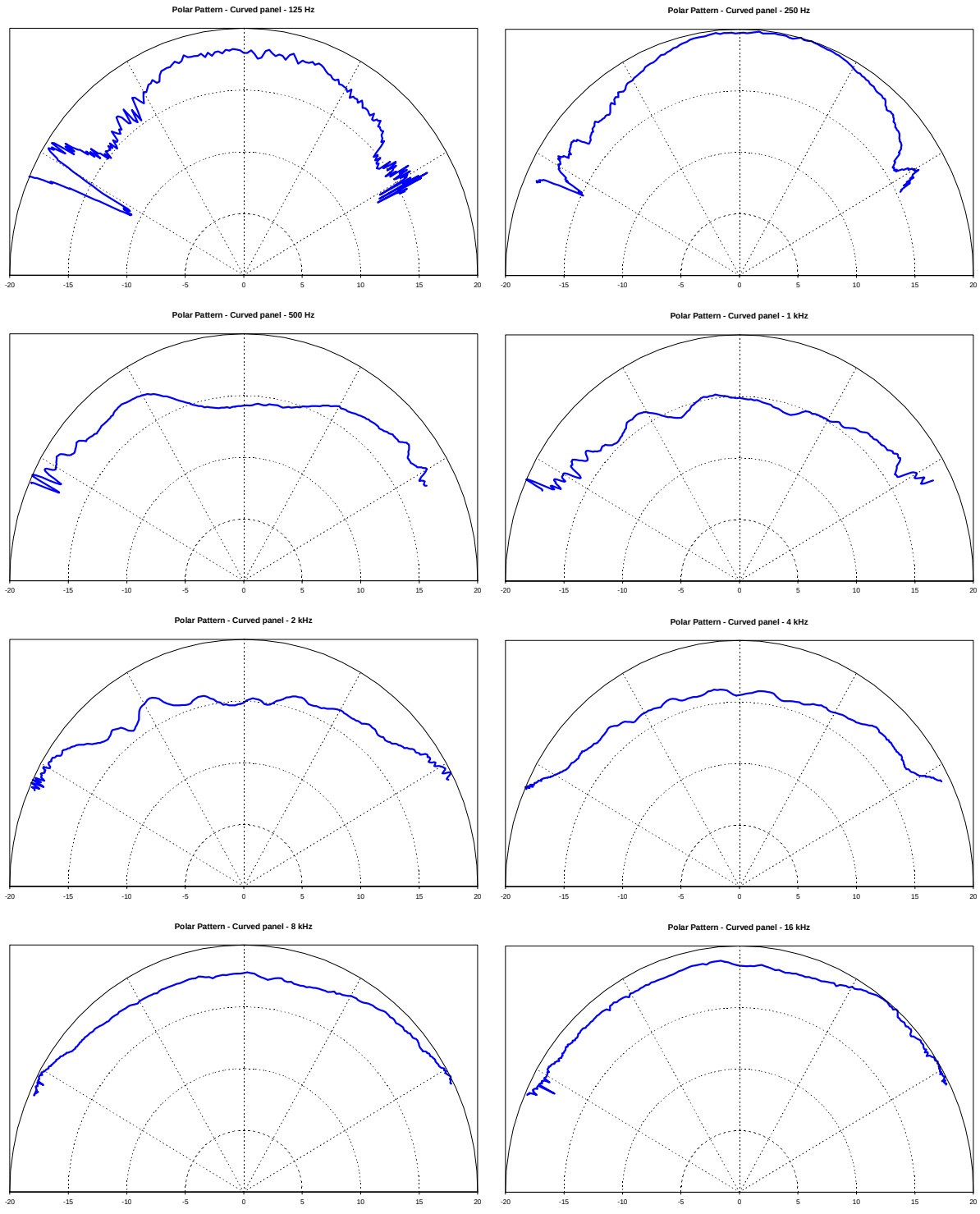

Fig. 15 – Polar patterns of the curved panel

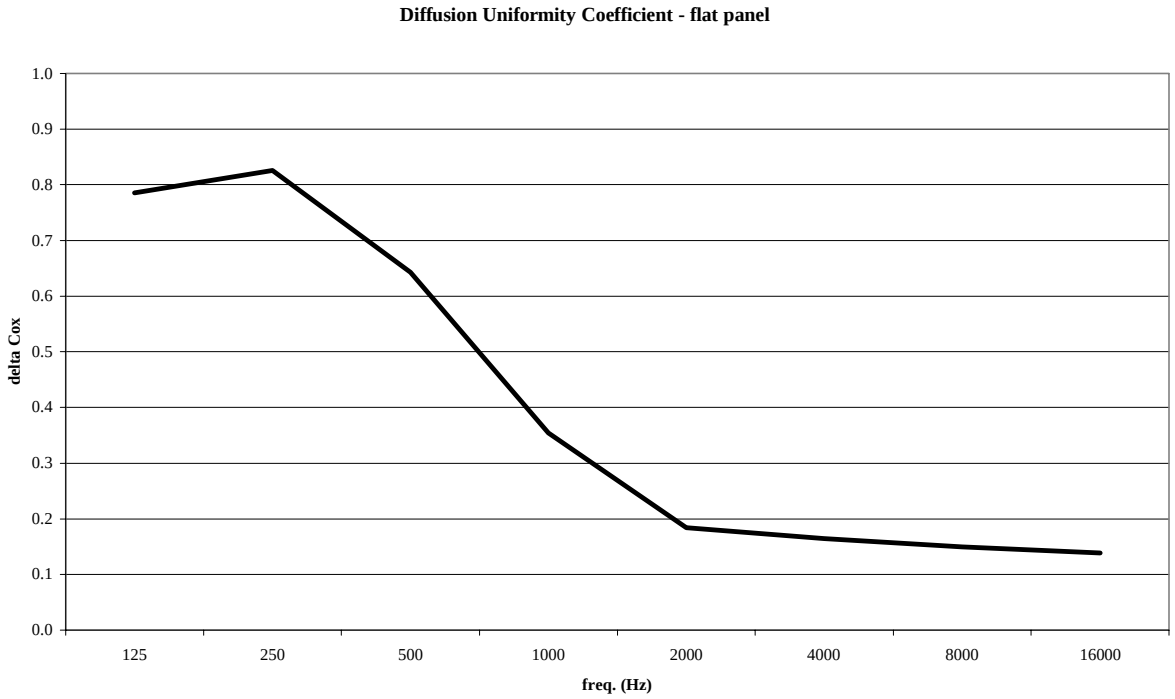

Fig. 16 – Values of δ_{uc} for the flat panel

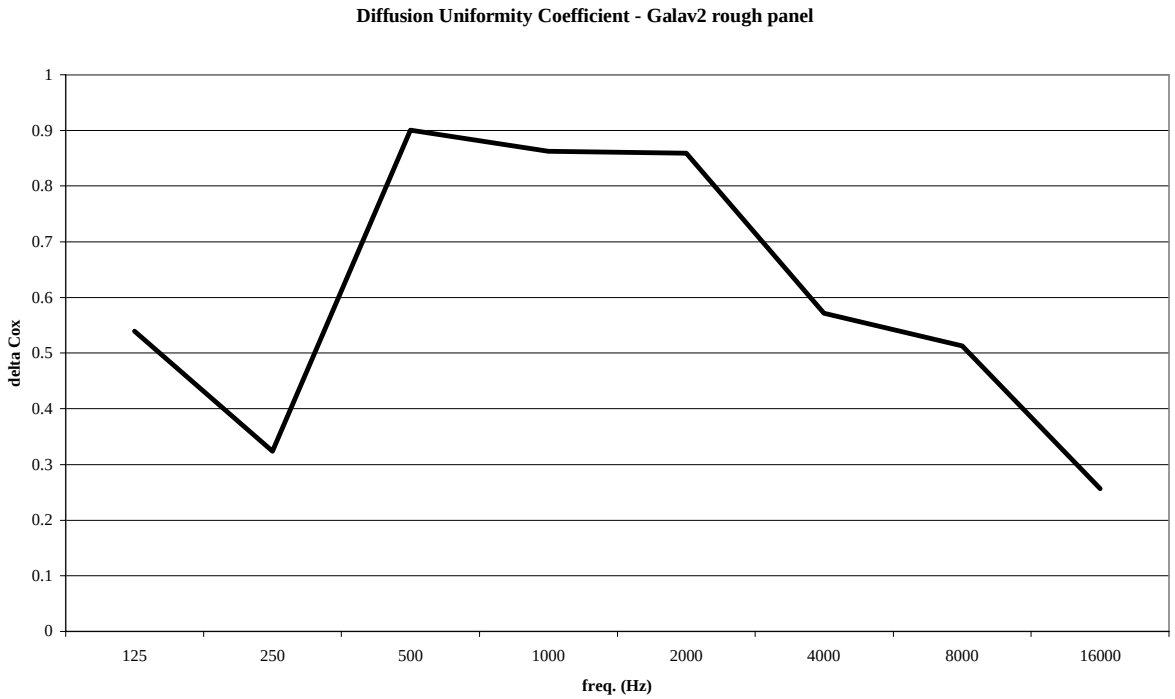

Fig. 17 - Values of δ_{uc} for the Galav2 diffusing panel

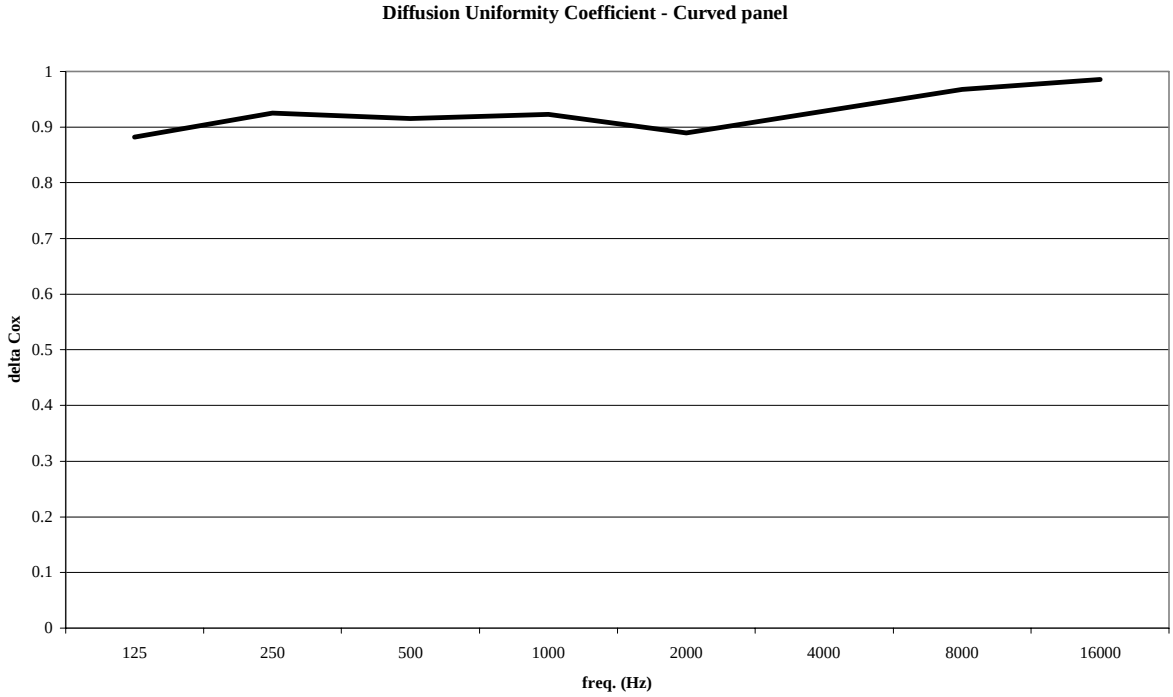

Fig. 18 - Values of δ_{uc} for the curved panel

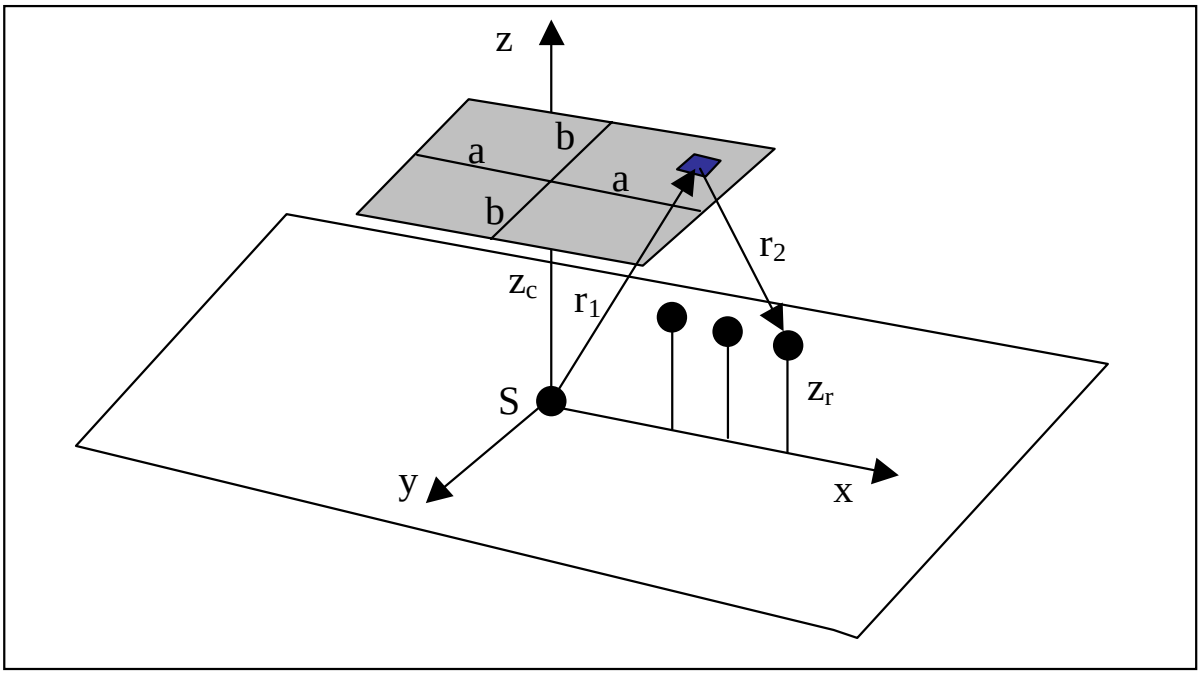

Fig. 19 – geometry for the theoretical computations

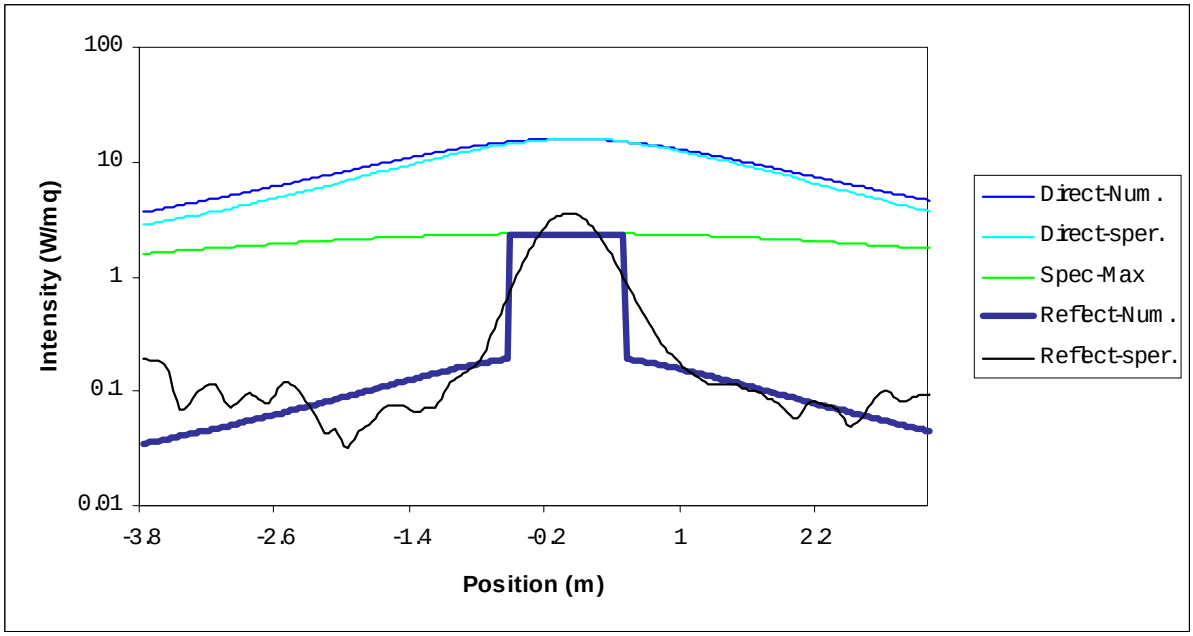

Fig. 20 – matching between numerical and experimental data – Flat Panel

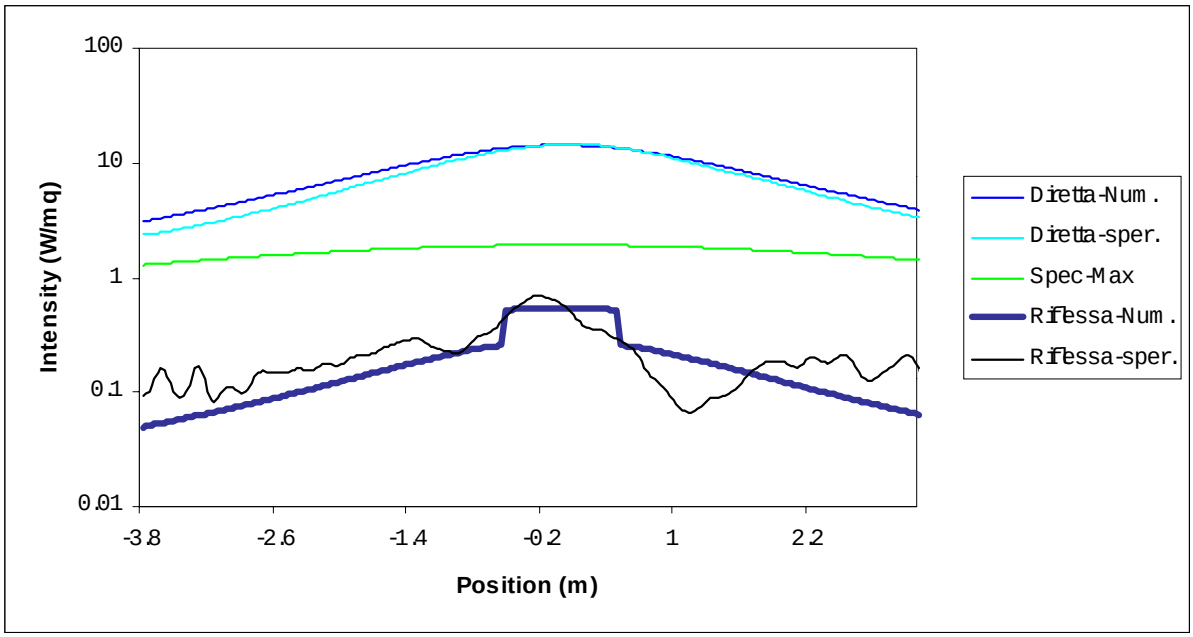

Fig. 21 – matching between numerical and experimental data – Galav2 diffusor

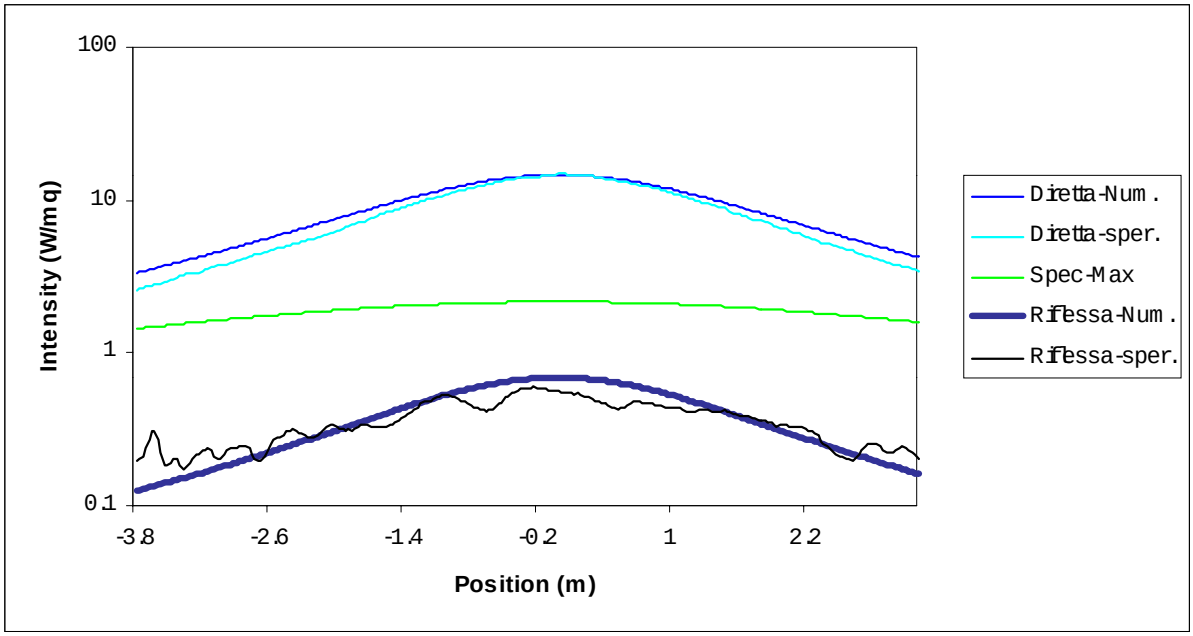

Fig. 22 – matching between numerical and experimental data – Curved Panel

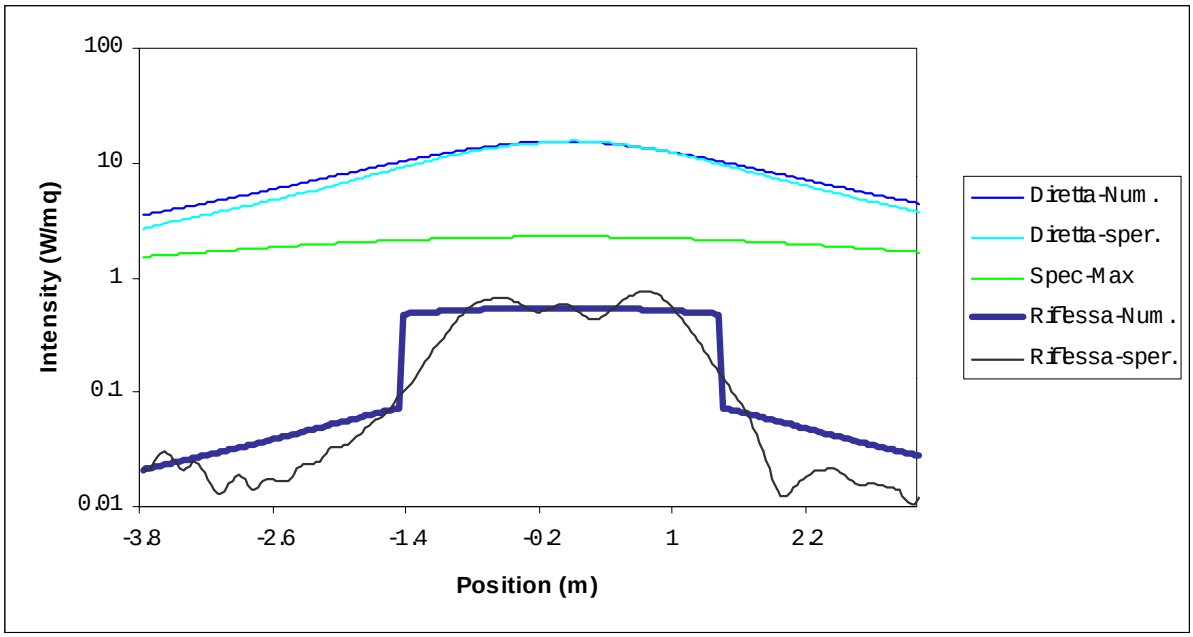

Fig. 23 – matching between numerical and experimental data – Curved Panel at 90°